

Development of a Liquid Crystal Based Sensor for Heavy Metal ion Detection

DIKSHA SHARMA

A dissertation submitted for the partial fulfilment of
BS-MS dual degree in Science



Indian Institute of Science Education and Research Mohali

April 2019

Certificate of Examination

This is to certify that the dissertation titled “Development of a Liquid Crystal Based Sensor for Heavy Metal ion Detection” submitted by Ms. **Diksha Sharma** (Reg. No. MS14044) for the partial fulfilment of BS-MS dual degree programme of the Institute, has been examined by the thesis committee duly appointed by the Institute. The committee finds the work done by the candidate satisfactory and recommends that the report be accepted.

Dr. Raj Kumar Roy Dr. Subhabrata Maiti Dr. Santanu K.Pal

(Supervisor)

Dated: April 26th, 2019

Declaration

The work presented in this dissertation has been carried out by me under the guidance of Dr. Santanu K. Pal at the Indian Institute of Science Education and Research Mohali.

This work has not been submitted in part or in full for a degree, a diploma, or a fellowship to any other university or institute. Whenever contributions of others are involved, every effort is made to indicate this clearly, with due acknowledgement of collaborative research and discussions. This thesis is a bonafide record of original work done by me and all sources listed within have been detailed in the bibliography.

Diksha Sharma

(Candidate)

Dated: April 26, 2019

In my capacity as the supervisor of the candidate's project work, I certify that the above statements by the candidate are true to the best of my knowledge.

Dr. Santanu K. Pal

(Supervisor)

Acknowledgement

First and foremost I would like to thank my parents for their undeterred faith in me and for always being my pillar of strength. I cannot thank them enough for always believing in me and guiding me through each and every step of my journey. I would also like to thank my brother, who has been my role model and moral support since childhood.

I would like to thank all the teachers and members of IISER Mohali for making me the person I am today. I would always carry with me the lessons that I learnt here. IISER Mohali would always have a special place in my heart.

Along with this, I thank my supervisor Dr. Santanu K. Pal for his constant guidance and support throughout the journey. This wouldn't have been possible if it were not for his helpful discussions and directions that resulted in successful execution of the project. I also thank Indu Verma, Dr. Manisha Devi and Dr. Rajib Nandi for their collaboration and expertise.

Apart from this, I thank my fellow MS labmates, Neha, Kaveri, Najiya and Abdul for making the journey a fun ride. I express my deep gratitude towards Ipsita Di, Vidhika Di and Supreet Di for being my undeclared mentors. I extend my thanks to Yogi Bhaiya, Shruti Di and Harpreet Bhaiya for being my refuge from a hectic day at lab, it wouldn't have been possible without those refreshing breaks with you. I thank Nazma Mam, Golam Sir, Varsha Di, Indu Bala Di, Joydip Bhaiya, Madhu and all lab members for providing a conducive lab environment and all the possible help in the lab.

And last but not the least, I thank all my friends and give a big shoutout to Tejasi and Avneet for being with me through all the ups and downs during my stay at IISER Mohali. Most of my sweet and fun memories constitute of you two. I also thank Vaishnavi for always being there for me, I couldn't have asked for a better neighbour and friend.

Thank you everyone.

Diksha Sharma

Dedicated to my family and friends.

Contents

List of Figures	<i>iii</i>
List of Scheme.....	<i>v</i>
Notation	<i>vi</i>
Abstract	<i>vii</i>
1 Introduction	
1.1 Basic Theory	2
1.2 Experimental Section	8
1.2.1 Materials	8
1.2.2 Methods	9
1.2.2.A Fabrication of glass microscope slides with DMOAP ..	9
1.2.2.B Preparation of LC thin films.....	9
1.2.2.C Preparation of the aqueous solutions used during the experiments.....	10
1.2.2.D Optical Characterization of LC films	11
2 Results and Discussions	
2.1 Optimization of CTAB Concentration	13
2.2 Optimization of Aptamer Concentration	15
2.3 Effect of Pb ²⁺ ions on the System.....	17
2.4 Determining Detection Limit of the Pb ²⁺ ions.....	17

2.5 Selectivity of the LC Sensor.	19
2.6 Specificity of the Sensor towards Aptamer	21
2.7 Comparison with the existing methods of lead ion Detection.	21
3 Summary and Conclusions	
3.1 Conclusion	24
3.2 Future Outlook.	25
Bibliography.	26

List of Figures

Figure 1 Molecular structures of commonly used reagents in the experiments A) DMOAP (N,N-dimethyl-N-octadecyl-3-aminopropyltrimethoxysilyl chloride) B) 5CB (4-Cyano-4'-pentylbiphenyl) C) HEPES Buffer (2-[4-(2-hydroxyethyl) piperazin-1-yl]ethanesulfonic acid) D) CTAB (Hexadecyltrimethylammonium Bromide)

Figure 2 Polarized optical microscope (POM) images of 5CB film hosted within a gold TEM grid on a DMOAP functionalized glass substrate before and after introduction of 1mM HEPES buffer (pH 7.4).

Figure 3 POM images of 5CB in gold TEM grid on DMOAP coated glass slide after introduction of 7 μ M CTAB and 5 μ M CTAB after 0.5 and 20 min of addition of CTAB.

Figure 4 POM images of 5CB in gold TEM grid on DMOAP coated glass slide after 0.5 and 20 min of introduction of 150 nM and 200 nM of SRNA pre-incubated with 7 μ M CTAB.

Figure 5 POM images of 5CB in gold TEM grid on DMOAP coated glass slide before and after introduction of 300 nM Pb^{2+} to the system.

Figure 6 POM images of 5CB in gold TEM grid on DMOAP coated glass slide after introduction of 30, 10, 3 and 1.5 nM pre-incubated Pb^{2+} , 200 nM SRNA and 7 μ M CTAB.

Figure 7 (A) Plot showing correlation between concentration of Pb^{2+} ions and average gray scale intensity after 20 minutes of addition of solution. (B) Graph representing average gray scale intensity vs time for different concentrations of Pb^{2+} ions.

Figure 8 POM images of 5CB in gold TEM grid on DMOAP coated glass slide after introduction of 75 nM pre-incubated Co^{2+} , Hg^{2+} , Ni^{2+} , Zn^{2+} and Pb^{2+} , 7 μM CTAB and 200 nM SRNA. Scale bar = 200 μm .

Figure 9 (A) Plot showing correlation between 75 nM concentration of different metal ions and average gray scale intensity after 20 minutes of addition of solution. (B) Graph representing average gray scale intensity vs time for different metal ions.

Figure 10 POM images of 5CB-aqueous interface laden with 7 μM CTAB and 150 nM Pb^{2+} with A) 200 nM SRNA aptamer sequence (specific) B) 200 nM random aptamer (non-specific).

List of Schemes

Scheme 1 Schematic illustration of the temperature dependent phases of a Liquid Crystalline material.

Scheme 2 Schematic illustration of the surface director and the direction of the easy axis of LC on the interface.

Scheme 3 Schematic demonstrating the proposed design for label free aptamer based LC sensor for detection of Pb^{2+} ions based on self-assembly of CTAB at interface influenced by conformational changes in aptamer upon binding with the target ion.

Scheme 4 Schematic illustration of the system used for creating an LC-aqueous interface.

Notation

LC	Liquid Crystal
RNA	Ribonucleic Acid
DNA	Deoxyribonucleic Acid
5CB	4-Cyano-4'-pentylbiphenyl
DMOAP	N,N-dimethyl-N-octadecyl-3-aminopropyltrimethoxysilyl chloride
CTAB	Hexadecyltrimethylammonium Bromide
HEPES	2-[4-(2-hydroxyethyl) piperazin-1-yl]ethanesulfonic acid
SRNA	Spinach RNA
Fig.	Figure
Min.	Minutes
<i>GI</i>	Gray Scale Intensity
SELEX	Systematic Evolution of Ligands by Exponential enrichment
POM Images	Polarized Optical Microscope Images

Abstract

We report a simple, label free and sensitive detection of lead (Pb^{2+}) ions using liquid crystals (LCs) with a detection limit of 3 nM. The LC-aqueous interface is initially decorated with a positively charged surfactant, CTAB (Hexadecyltrimethylammonium Bromide) which aligns the LC homeotropically through the hydrophobic interactions between LC and CTAB molecules. An ordering transition in LC is registered on the addition of Spinach RNA (SRNA) (from homeotropic to planar) due to interaction of SRNA and CTAB leading to the disruption of the self-assembled monolayer of CTAB. Again, we observed an ordering transition of the LC (from planar to homeotropic) upon contact of Pb^{2+} ions with SRNA-CTAB complexes. The reported system exhibits an excellent detection limit of 3 nM Pb^{2+} ions. This is far below the permissible limit of Pb^{2+} in potable water (72 nM). It also shows high selectivity towards Pb^{2+} over other ions. The system also shows a specificity towards SRNA over other RNA sequences. These properties make the proposed system a promising candidate for Pb^{2+} ion detection in point of care applications.

Chapter 1

Introduction

1.1 Basic Theory

1.2 Experimental Section

Introduction

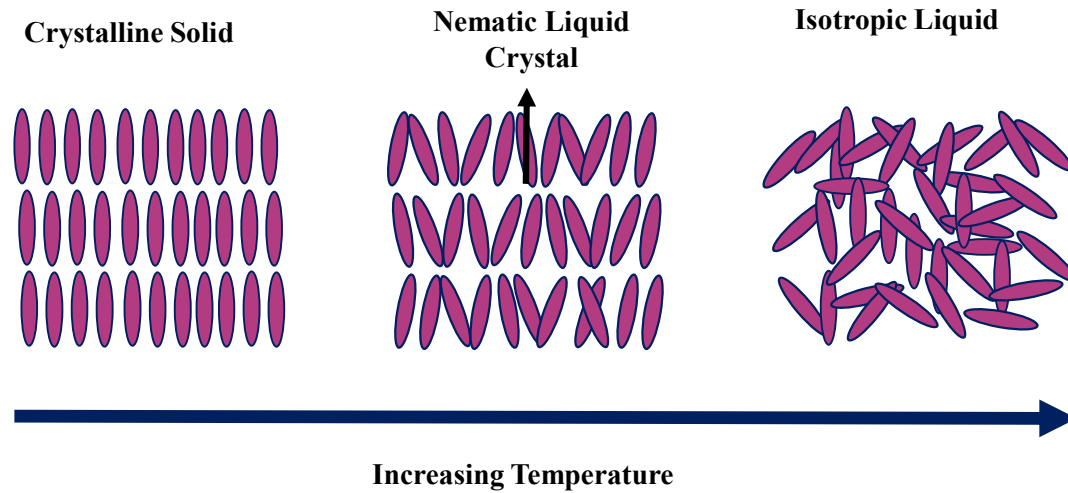
1.1 Basic Theory

Liquid crystals (LCs) are defined as state of matter possessing properties intermediate between that of solids and liquids. The solids have a rigid structure, with fixed positional and orientational order. On the other hand, liquids are relatively less rigid and possess no positional and orientational order. The LCs, however, possess very less or no positional order but have an orientational order. The LC molecules are oriented along a fixed direction known as the director of the LC molecules. The liquid crystalline molecules possess some properties similar to that of liquids such as fluidity, formation of droplets, etc. and some properties similar to solids like birefringence, anisotropy, and more. There are several types of LC molecules with the most common being the calamitic LCs wherein the molecular axis is much longer than the other two axes, imparting anisotropy to the molecules. The other type of LCs is discotic LC. In both calamitic and discotic LCs the LC phase is observed as a function of temperature. On the other hand, in lyotropic LCs the LC phase is observed in presence of some solvent.¹

The simplest phase of the calamitic LCs is the nematic phase where the molecules possess an orientational order but no positional order. The molecules are oriented towards a preferred direction known as the director of the LC molecules. Scheme 1 shows the transition from crystalline solids to nematic LC to isotropic liquid on increasing the temperature going from a highly ordered crystalline structure to relatively less ordered nematic phase and then to highly random isotropic phase.¹

Such thermotropic LCs possessing a long range orientational order amplify and transfer the molecular level information from the interface.²⁻²¹ This interfacial interaction and information transfer leads to orientational changes upto 1-100 μm from the interface within the LC.²⁻⁶ Owing to the birefringence of the LCs, polarized optical microscopy enables easy characterization of different director profiles. In homeotropic orientation of the LC, the light passes through the LC undeflected and the analyser being perpendicular to the polarizer blocks the light imparting a dark optical appearance.

Whereas in the planar orientation, when the light passes through the LC, it gets deflected and there is a component of the light parallel to the analyser making it appear bright.



Scheme 1. Schematic illustration of the temperature dependent phases of a LC material. (Redrawn from [21])

The interaction of the LC with a surface govern the orientation of the LC which results into the surface-induced anchoring, known as the surface anchoring of the LCs. The orientation of director having the lowest free energy is known as the ‘easy axis’ of the LC. The change in the director orientation is caused by the external stimuli the LC in contact with the surface gets from its environment, which leads to the dependence of free energy on the orientation of the interface.²¹ (Scheme 2) The orientation dependence of the interfacial energy is governed by

$$\sigma = \sigma_0 + \frac{1}{2} W_a \sin^2(\theta_d - \theta_0)$$

(Reproduced from [21])

where

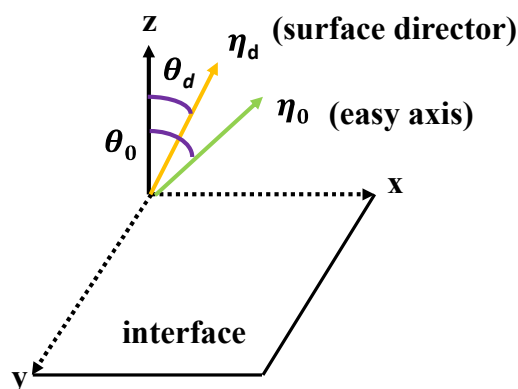
σ : Interfacial free energy

σ_0 : Part of interfacial free energy independent of orientation

W_a : Anchoring energy

θ_d : Orientation of the surface director

θ_0 : Orientation of the easy axis.



Scheme 2. Schematic illustration of the surface director and the direction of the easy axis of LC on the interface. (Redrawn from [21])

Distinct director profiles generate distinct optical appearances of the LC. Exploiting this ability of the LC to sensitively detect small changes in its environment, several label free LC based biosensors have been developed. Biochemical events like DNA adsorption¹⁰ and hybridisation⁹, aptamer-small molecule binding¹¹, cell adhesion^{13,14}, protein adsorption^{3,15-18}, antigen-antibody binding^{19,20}, enzymatic reactions, etc. have been detected using the interfaces formed between LC and aqueous phases^{21,23}. Such macromolecular binding events at the interface trigger an orientational transition in the LC which further amplifies and enables the detection of an event occurrence or the target analyte (upto nanomolar concentrations). The detection of a toxic heavy metal ion using LC in an aqueous phase faces the challenges of poor selectivity, specificity and high detection limits.²⁴⁻²⁶ The high mobility of the metal ions in the bulk phase and similar charge to radius ratio of several metal ions further cause hindrance in developing an LC based biosensor for heavy metal ions in the aqueous phase. So the system poses a problem in the case of the aqueous phase. However oligonucleotides based recognition of Hg (II) ions has enabled a detection limit of 0.1 nM target

concentrations. But the design is complex as it involves three oligonucleotides probes to generate an optical signal.²⁷ Here, we attempt to develop a simple aptamer based LC sensor to detect the target analyte (heavy metal ion) upto nanomolar concentrations in aqueous phase.

Aptamers are nucleic acids that are being heavily investigated. These are small single stranded RNA/DNA molecules which are capable of binding specifically with proteins or heavy metal ions. The nucleic acid sequences as molecular recognition element offer exceptional affinity towards the target and several other advantages such as simple design, stability in aqueous solution and cost effective synthesis.²⁸ This binding often leads to changes in the secondary or tertiary structures of the aptamers. The change in the secondary or tertiary structures have been previously exploited to design sensors of different types.²⁹ The principle for detection used in such biosensors is often associated with change in conformations such as formation of a duplex or a G-quadruplex upon binding with the target.²⁹ The change in the structure of the RNA/DNA aptamers are easily detectable using circular dichroism or fluorescence studies. Discovered in early 1990s, aptamers have been exploited clinically marking their relevance for diseases like HIV, cancer and macular degeneration.

SELEX (Systematic Evolution of Ligands by Exponential enrichment) is used for selecting aptamers, which was first reported in 1990. To start with, the method takes a random sequence library of single-stranded DNA (ssDNA) or single-stranded RNA (ssRNA) of lengths 20-100 nucleotides. Then all these random sequences are flanked with the constant sequence required for capturing the target. This initial pool of aptamers is then exposed to the target proteins or molecules and then change in the sequence of some aptamers occur in order to bind with the target. Further, the aptamers which do not bind with the target are washed away and the ones with high affinity towards the target are enriched by polymerase chain reaction (PCR) amplification or reverse transcriptase-PCR (RT-PCR) for DNA aptamers and RNA aptamers respectively, followed by *in vitro* transcription. This pool of aptamers is again exposed to the target and the whole process is repeated. Counter selection of the aptamers can also be done by introducing some unwanted targets and then depleting the aptamers which bind with them (i.e. getting rid of the non-specific aptamers). After several rounds of selection and enrichment, the pool of aptamers obtained shows an increased binding affinity towards the target molecules and will converge to one or a few final

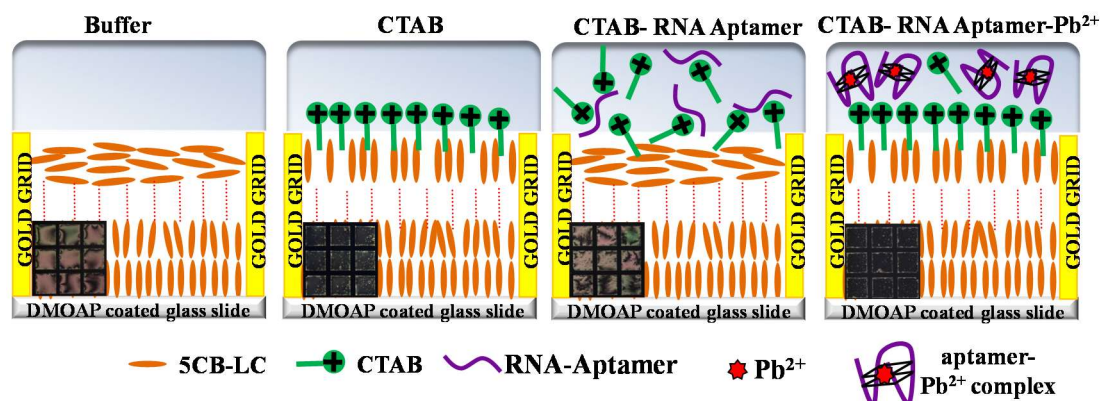
sequences. In the end, clones of the consensual aptamers can be generated and tested for target binding affinity and specificity.²⁸

These target specific aptamers have been employed to develop biosensors of different types using different techniques such as fluorescence, calorimetry, electrochemical methods etc. These techniques, however, impose certain limitations such as high equipment costs, need of fluorophores, expert handling and aptamer immobilization. To overcome such limitations there is a need to develop a simple, easy to visualize sensor in the aqueous phase to detect the heavy metal ions.

It has been previously reported that the interfacial adsorption of oligonucleotides can trigger change in LC orientation at the LC-aqueous interface driven by non-covalent intermolecular interactions. However, at the surfactant laden LC-aqueous interfaces, the electrostatic as well as hydrophobic interactions between nucleobases and LC molecules govern the ordering of LC.⁹⁻¹² Hence, DNA and biomolecules bound DNA induce different LC orientation at the cationic surfactant-laden interface. Exploiting these known results we explored whether it is possible to design an aptamer based LC sensor for detection of heavy metal ions at the surfactant laden LC-aqueous interface.

Heavy metals with their marked presence in the ecosystem and the inherent toxicity pose a threat to the environment and to human health because of constant exposure and abundance. Heavy metals are considered one of the major sources of pollution in the environment. Among these, Pb^{2+} is the second most abundant toxic heavy metal. Small amount of Pb^{2+} can lead to several diseases ranging from nervous system dysfunction, anaemia, reproductive dysfunction and development disorders to death in extreme cases of exposure to high concentrations. Even though Pb^{2+} containing gasoline and paints have been banned in some countries, the other sources of Pb^{2+} contamination like batteries, alloys and anti-corrosion coatings are still prevalent. Among others it is a major source of soil and ground water pollution.³⁰⁻³² This prevalence of Pb^{2+} then leads to introduction of lead ions into the water bodies from where it finds its way to human consumption. The maximum permissible limit of Pb^{2+} concentration in the potable water as defined by the world health organisation is 72 nM³³, but it has been found that drinking water at a lot of places around the world contain Pb^{2+} concentration exceeding this limit of permissibility. The abundance of Pb^{2+} along with its potential health risks calls for an efficient and cost-friendly method for Pb^{2+} ion detection. Several attempts have been made in the past towards the detection of Pb^{2+} ions. Traditional methods of

Pb²⁺ ion detection such as fluorescence, inductively coupled plasma mass spectroscopy (ICP-MS) among others require expensive instrumentation, expert handling and sophisticated analysis. We intend to find a simple, easy to visualize and effective way of Pb²⁺ ion detection using LCs.



Scheme 3. Schematic demonstrating the proposed design for label free aptamer based LC sensor for detection of Pb²⁺ ions based on self-assembly of CTAB at interface influenced by conformational changes in aptamer upon binding with the target ion. (Inset images: Polarized optical micrographs corresponding to respective interfacial event at LC-aqueous interface)

In the proposed system, we decorate the LC-aqueous interface with a self-assembly of a cationic surfactant, cetyltrimethylammonium bromide (CTAB) which imparts homeotropic anchoring to the LC through the hydrophobic interaction between hydrocarbon tails of the CTAB. On addition of negatively charged aptamer, the self-assembly of the CTAB at the interface gets disturbed due to the interaction between CTAB and aptamer which leads to planar alignment of LC.^{2,9} However, upon introduction of heavy metal ions into the system, we hypothesized that conformational changes get induced in the aptamer. This would decrease the interfacial coverage of aptamer at the interface and hence promote the CTAB-LC coupling to result into homeotropic ordering in the LC. (Scheme 3) Herein we test this hypothesis to report a simple LC based method for Pb²⁺ ion detection using Spinach RNA (SRNA) as a recognition probe.

1.2 Experimental Section

1.2.1 Materials:

Spinach RNA:

5'-

GGGGAGAAGGACGGGUCCAGUGCGAAACACGCACUGUUGAGUAGAGUG
UGAGCUCCC-3'

Random RNA sequence:

GGGAGGACGAUGCGGAUCAGCCAUGUUUACGUCACUCCUUGUCAAUCC
UCAUCGGC

The RNA sequences were customized and purchased from Integrated DNA Technologies and used without further purification.

Sulfuric acid, hydrogen peroxide (30% *w/v*) and metal salts like lead (II) acetate trihydrate (Pb^{2+}) and mercury (II) chloride were obtained from Merck (Mumbai, India). Metal salts nickel (II) chloride hexahydrate, cobalt (II) acetate tetrahydrate and zinc (II) acetate dihydrate were obtained from Alpha Aesar. 4-Cyano-4-pentylbiphenyl (5CB), N,N-dimethyl-N-octadecyl-3-aminopropyltrimethoxysilyl chloride (DMOAP), cetyltrimethylammonium bromide (CTAB), hydrochloric acid (HCl), sodium hydroxide (NaOH) and HEPES [4-(2-hydroxyethyl)-1-piperazineethanesulfonic acid] were obtained from Sigma-Aldrich (St. Louis, MO). (Fig. 1) Ethanol was obtained from Changshu Hongsheng Fine Chemical Co., Ltd. Milli-Q-system (Millipore, Bedford, MA) was used to deionise distilled water (DI water). Glass microscopic slides of finest Premium grade were purchased from Fischer Scientific (Pittsburgh, PA). Transmission electron microscopy gold grids (283 μm grid spacing, 20 μm thickness, 50 μm wide bars) were acquired from Electron Microscopy Sciences (Fort Washington, PA). Diamond glass cutter was obtained from sigma.

1.2.2 Methods

A) Fabrication of glass microscope slides with DMOAP:

The glass slides were cleaned with piranha solution and then fabricated with DMAOP as per the previously reported procedures.²

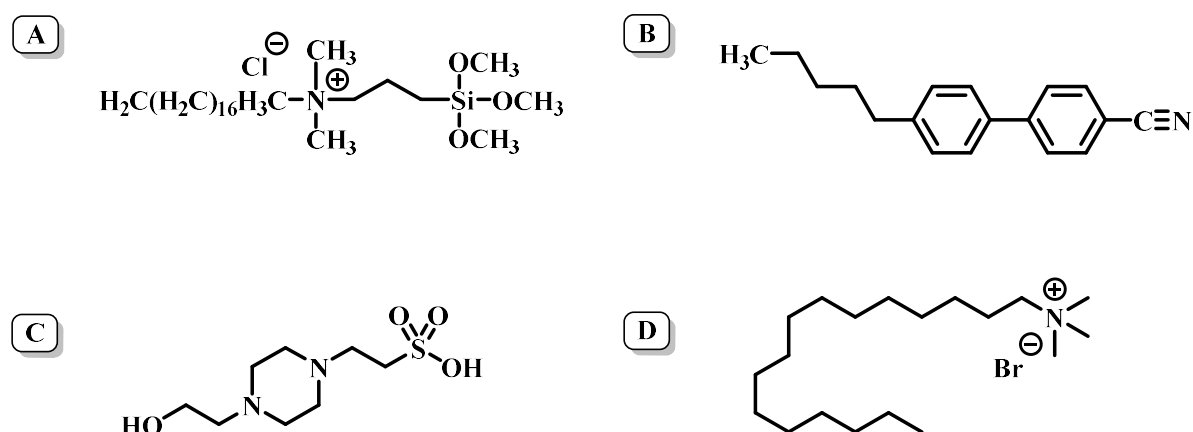
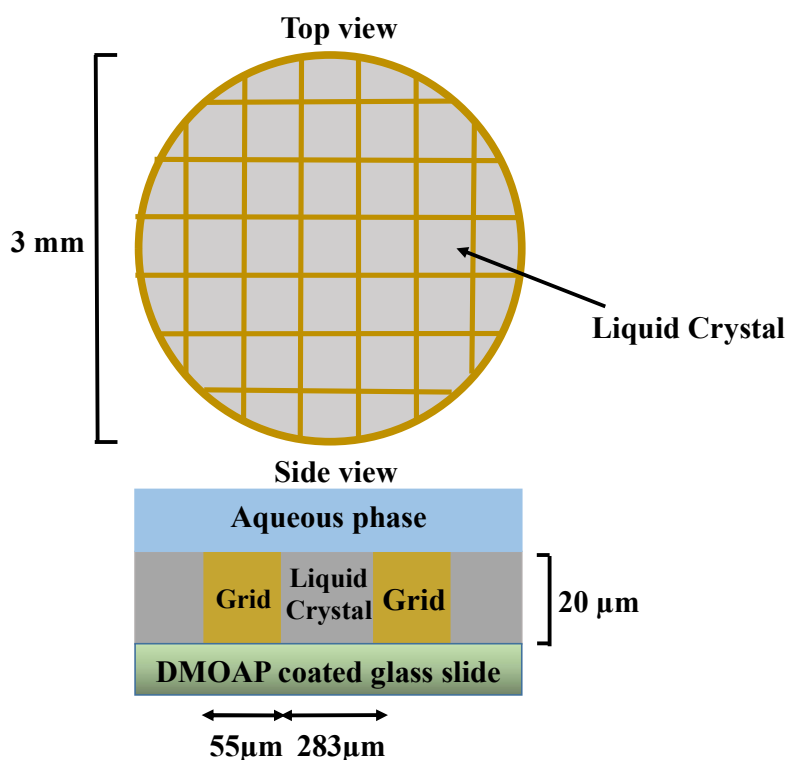


Figure 1. Molecular structures of commonly used reagents in the experiments A) DMOAP (N,N-dimethyl-N-octadecyl-3-aminopropyltrimethoxysilyl chloride) B) 5CB (4-Cyano-4'-pentylbiphenyl) C) HEPES Buffer (2-[4-(2-hydroxyethyl) piperazin-1-yl]ethanesulfonic acid) D) CTAB (Hexadecyltrimethylammonium Bromide)

B) Preparation of LC thin films²:

DMOAP coated glass slides were cut into small square shaped slides of around 1.5 X 1.5 cm² dimension using a diamond glass cutter. These small square shaped slides were purged with gaseous N₂ to get rid of the small glass particles from the surface. Further, clean gold TEM grids were put onto the DMOAP-coated 1.5 X 1.5 cm² square slides and filled with 5CB. The extra LC was removed using the Hamilton syringe in order to get a uniform interface. DMOAP through its hydrophobic interaction aligns the LC molecules perpendicularly and provides a strong homeotropic anchoring of the LC at the LC-glass interface resulting into a dark appearance under crossed polarizers.² 100 μL of the aqueous solution of interest was poured onto the TEM grid on the glass slide

using a micropipette which takes a droplet like form because of the hydrophobic surface of the glass that supports the non-wetting of the surface. This was followed by observation of the TEM grid under polarized optical microscope. (Scheme 4)



Scheme 4. Schematic illustration of the system used for creating an LC-aqueous interface. (Redrawn from [21])

C) Preparation of the aqueous solutions used during the experiments:

1 mM 2-[4-(2-hydroxyethyl) piperazin-1-yl]ethanesulfonic acid (HEPES) buffer was freshly prepared by dissolving a calculated amount of HEPES solid in Millipore water and the pH was adjusted to 7.4 using a pH meter. All the solution were then prepared in 1 mM HEPES buffer (pH 7.4). Stock solutions of CTAB (1mM) and all the metal ions (9 μM) were prepared by dissolving the calculated amount of the respective solid powder in 1mM HEPES (pH 7.4) at room temperature. Aptamer was diluted from the stock solution of concentration 2.4 μM prior to use. In order to prepare a complex of CTAB and aptamer calculated amounts of solutions were mixed to get the desired final concentrations and then incubated for 30 minutes. To detect Pb²⁺ ions, calculated

amount of Pb^{2+} solutions were incubated with aptamer for one hour followed by addition of CTAB solution yielding the final desired concentration of Pb^{2+} ions and $7\mu\text{M}$ CTAB and 200 nM aptamer. After 30 minutes of adding CTAB, the solution was added onto the LC grid and then observed under the polarized optical microscope. Similar procedure was followed with other heavy metals for selectivity experiments.

D) Optical Characterization of LC Films

The ordering of LC and their director profiles were characterized by observing the LC film under Zeiss polarising microscope equipped with crossed polarizers. The LC film was observed under a 50X objective power and all the images were captured using an AxioCam camera.

Chapter 2

Results & Discussions

- 2.1 Optimization of CTAB Concentration
- 2.2 Optimization of Aptamer Concentration
- 2.3 Effect of Pb^{2+} ions on the System
- 2.4 Determining Detection Limit of the Pb^{2+} ions
- 2.5 Selectivity of the LC Sensor
- 2.6 Specificity of the Sensor towards Aptamer
- 2.7 Comparison with the existing methods of Pb^{2+} ion Detection

Results and Discussions:

Cetyltrimethylammonium bromide (CTAB), a positively charged surfactant, when introduced onto an LC-aqueous interface led to a homeotropic orientation of LCs, imparting a dark appearance to the system when observed under the crossed polars of the polarized optical microscope. The homeotropic anchoring of the LC is attributed to the hydrophobic interactions between the hydrocarbon tails of the LC and CTAB. CTAB being positively charged, can interact with the negatively charged nucleobases electrostatically which can then further interact with the LC at the aqueous interface and hence impart a planar alignment. However, in presence of Pb^{2+} , the second most toxic heavy metal, we hypothesized that RNA which would interact with the Pb^{2+} ions, forming a complex which might lead to coupling of CTAB with the LC at the aqueous interface resulting into homeotropic orientation. For this purpose, we used the Spinach RNA which has a specific affinity for Pb^{2+} due to formation of a G-quadruplex.³⁴ To test this hypothesis we (work done in collaboration with Indu Verma, Manisha Devi and Rajib Nandi) conducted the experiments with different concentrations of Pb^{2+} ions and with other heavy metal ions to confirm the selectivity of the system.

2.1 Optimization of CTAB concentration

At first we sought to study the response of the LC in presence of different concentrations of cetyltrimethylammonium bromide (CTAB) at the LC-aqueous interface. For this, 4-cyano-4-pentylbiphenyl (5CB) was confined with the TEM gold grids which were supported on the N,N-dimethyl-n-octadecyl-3-aminopropyltrimethoxysilyl chloride (DMAOP)-coated glass slides. DMAOP at the bottom and air at the top interface impart a homeotropic alignment to 5CB which results in a dark appearance when observed under crossed polars. As a control we added 1mM HEPES buffer to the LC film which resulted in a bright optical appearance. (Fig. 2) The results are consistent with the planar alignment of the LC molecules in presence of water.

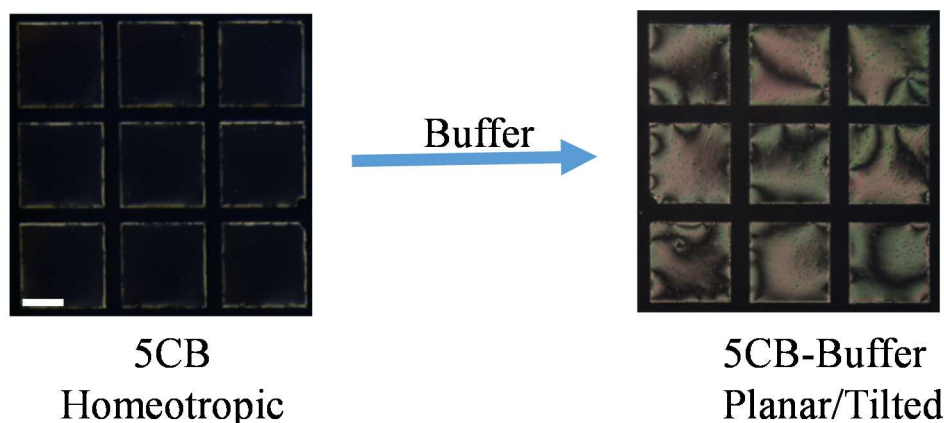


Figure 2. Polarized optical microscope (POM) images of 5CB film hosted within a gold TEM grid on a DMOAP functionalized glass substrate before and after introduction of 1mM HEPES buffer (pH 7.4). Scale bar = 200 μm .

Further, we added an aqueous solution of CTAB and it was found that at a sufficiently high concentration of CTAB, the 5CB exhibited a homeotropic orientation. The dark optical response of LC in the presence of CTAB is due to the self-assembly of the CTAB molecules at aqueous-LC interface and because of the hydrophobic interaction between CTAB and LC hydrocarbon chains.² Next, we added different concentrations of CTAB solutions on the LC film to determine the minimum concentration required for the LC to exhibit the homeotropic alignment. To this respect, we conducted the experiment with 10 μM , 7 μM , 5 μM and 3 μM concentrations of CTAB. We observed that with 10 and 7 μM CTAB the LC showed a homeotropic orientation just after the addition of the solution, with 5 μM CTAB it took a little over 20 minutes for the LC to get aligned homeotropically whereas with 3 μM of CTAB the LC remained bright even after 30 minutes. Therefore, the minimum concentration required to get a homeotropic alignment was identified to be 7 μM as the LC showed dark appearance even after 30 minutes and hence 7 μM CTAB at pH 7.4 was used for all the further experiments. (Fig.3)

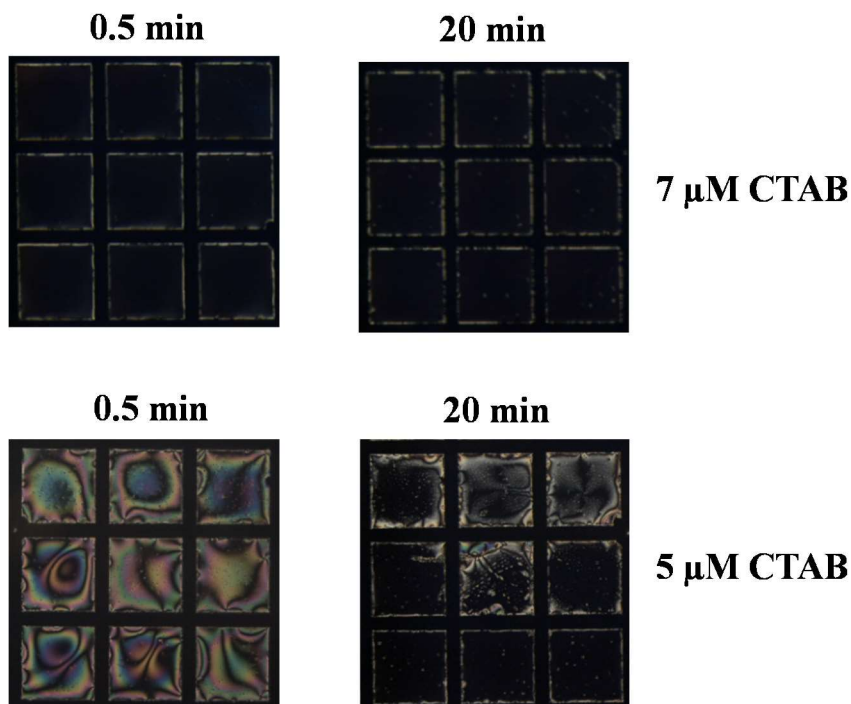


Figure 3. POM images of 5CB in gold TEM grid on DMOAP coated glass slide after introduction of $7 \mu\text{M}$ CTAB and $5 \mu\text{M}$ CTAB after 0.5 and 20 min of addition of CTAB.

2.2 Optimization of aptamer concentration

Next, we tried to find minimum concentration of aptamer required to bind with $7 \mu\text{M}$ CTAB so that the resultant solution when added to the LC film gives a planar alignment of the LC. Towards this, we took calculated amounts of SRNA and CTAB to give us the final desired concentrations in the mixture and incubated the mixture for 30 minutes. Since SRNA is negatively charged and CTAB is positively charged, there is an electrostatic interaction between the two. The strong electrostatic interactions between SRNA and CTAB disrupts the self-assembly of CTAB at the aqueous-LC interface resulting in a planar alignment of the LC.

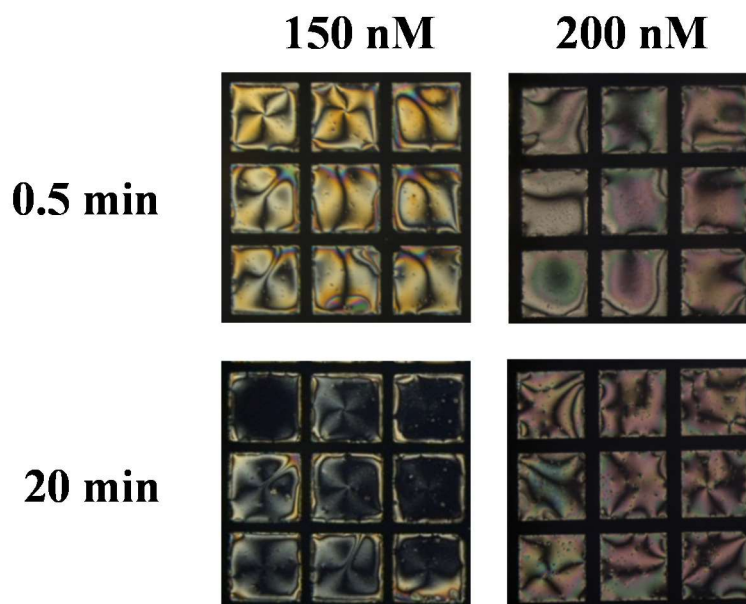


Figure 4. POM images of 5CB in gold TEM grid on DMOAP coated glass slide after 0.5 and 20 min of introduction of 150 nM and 200 nM of SRNA pre-incubated with 7 μ M CTAB.

At sufficiently high concentration of SRNA incubated with CTAB for 30 minutes, we obtained a planar orientation of the LC. Next we sought to determine the minimum concentration of SRNA required with 7 μ M CTAB to impart a planar orientation to the LC. For this, we incubated different concentrations of SRNA with CTAB for 30 minutes to get the desired concentration of SRNA and 7 μ M CTAB. After 30 minutes the solutions were introduced onto the LC film. It was observed that when solutions containing 300 and 200 nM of aptamer and 7 μ M of CTAB was added to the LC film, LC exhibited a planar orientation which was stable upto more than 30 minutes whereas with 150 and 100 nM of aptamer and 7 μ M CTAB the LC turned homeotropic in 30 and 20 minutes respectively. (Fig. 4) Therefore, a solution of 200 nM aptamer and 7 μ M CTAB was used for all the further experiments.

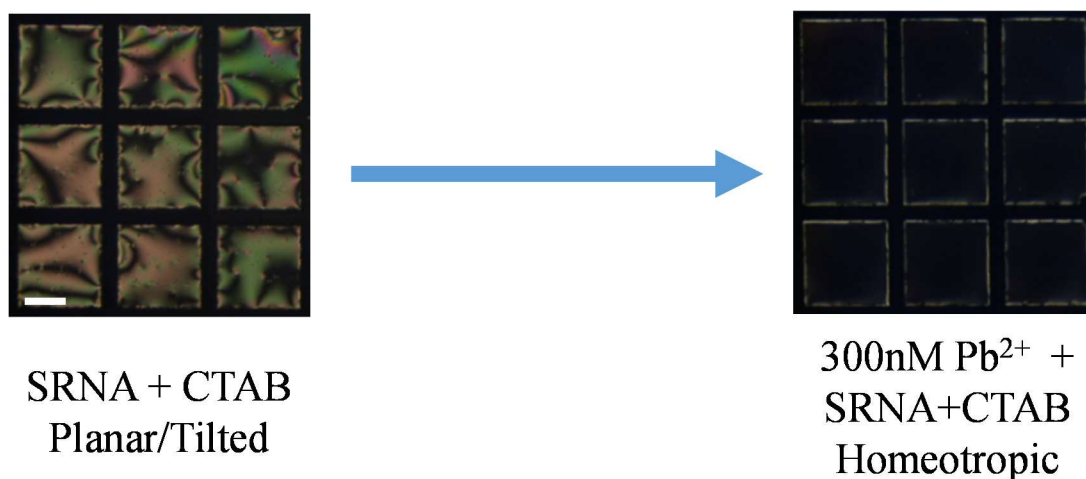


Figure 5. POM images of 5CB in gold TEM grid on DMOAP coated glass slide before and after introduction of 300 nM Pb^{2+} to the system. Scale bar = 200 μm

2.3 Effect of Pb^{2+} ions on the system

Our next step was to examine the effect of Pb^{2+} on our system. To that respect, we incubated a high concentration of Pb^{2+} (300nM) and 200 nM SRNA for 30 minutes and then added 7 μM of CTAB to the solution. After an hour of adding CTAB we introduced the solution on the TEM grid containing LC film. The orientation of LC turned homeotropic within 5 minutes of adding the solution. (Fig. 5) This indicated that the SRNA interacted with Pb^{2+} ions forming a G-quadruplex³⁴ which led to weakened interaction between SRNA and CTAB which further leads to self-assembly of CTAB at the LC-aqueous interface and hence a homeotropic orientation.

2.4 Determining detection limit of the Pb^{2+} ions

Our next motive was to determine the concentration of Pb^{2+} ions that can be detected using our system. To this respect, we incubated different concentrations of Pb^{2+} with SRNA for 1 hour and then added CTAB. The resultant solution was then added to the TEM grid containing 5CB after 30 minutes. It was made sure that the final concentration of SRNA and CTAB in the solution were 200 nM and 7 μM respectively. The final concentrations of the Pb^{2+} ions were kept at the desired values. The TEM grid was then observed for 30 minutes and we have reported the results upto 20 minutes. It was found that the LC turned dark within 20 minutes for concentrations upto 3 nM

(where most of the grids turned black and only a few were bright within the observed time period). For concentrations lower than 3 nM, the LC remained bright even after 30 minutes. (Fig. 6) This result depicts that the detection limit for Pb^{2+} ions for our system is 3 nM concentration, which is far below the maximum permissible limit of Pb^{2+} ions in water (72 nM).

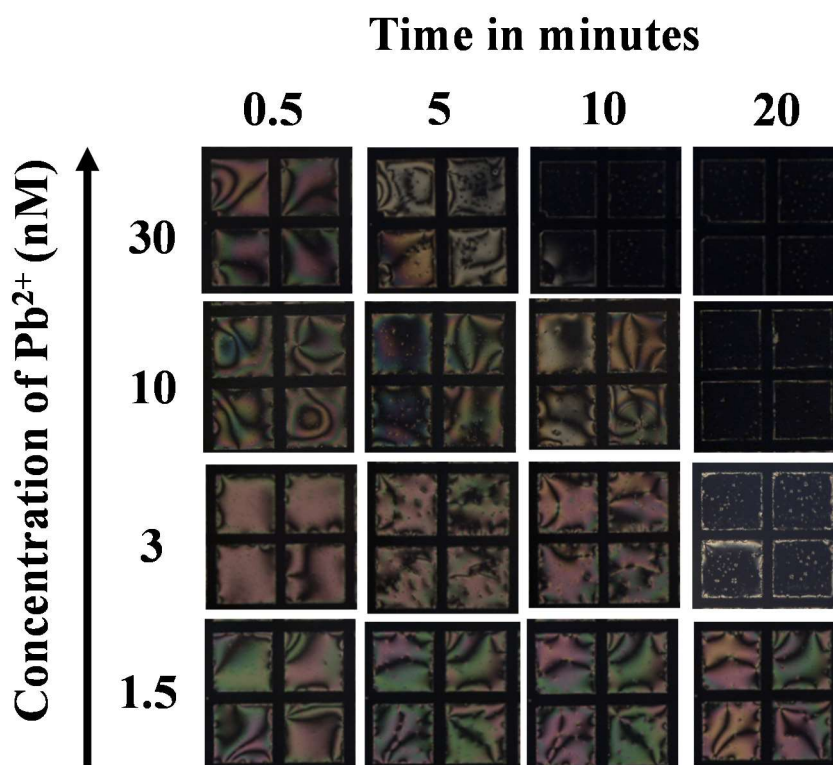


Figure 6. POM images of 5CB in gold TEM grid on DMOAP coated glass slide after introduction of 30, 10, 3 and 1.5 nM pre-incubated Pb^{2+} , 200 nM SRNA and 7 μ M CTAB.

This can also be observed by the correlation plot of Pb^{2+} concentration and the average gray scale intensity of the LC after 20 minutes. (Fig. 7A) The plot clearly shows the rapid decrease in the average gray scale intensity as the concentration of the Pb^{2+} ion increases, with the highest *GI* when there is no Pb^{2+} in the solution and attaining its constant minima after a given concentration of Pb^{2+} . The same gets reinforced with the average *GI* vs time plot for different concentrations of Pb^{2+} . (Fig. 7B) With time, there is a rapid plunge in the *GI* in case of solutions containing Pb^{2+} concentration equal to

or more than 3 nM (the detection limit of our system) whereas it remains almost constant for concentrations lower than that.

This suggests that our system can be used to detect Pb^{2+} ion concentration in potable water. The parameters used to judge a sensor are practical applicability, selectivity and specificity. With practical applicability being ticked off the list, we went on to see how our sensor fares on the other parameters.

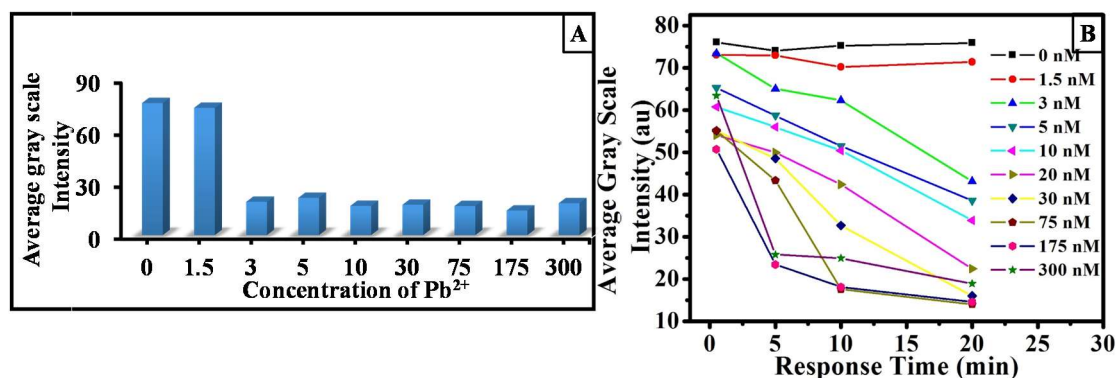


Figure 7. (A) Plot showing correlation between concentration of Pb^{2+} ions and average gray scale intensity after 20 minutes of addition of solution. (B) Graph representing average gray scale intensity vs time for different concentrations of Pb^{2+} ions.

2.5 Selectivity of the LC sensor

Next we went on to check the selectivity of the LC sensor towards Pb^{2+} ions. For this, we tested the response of our LC sensor towards the other prevalent heavy metal ions. For this we observed our system in presence of 75 nM of Co^{2+} , Ni^{2+} , Hg^{2+} and Zn^{2+} with an observation time of 20 minutes. We found that with all these metal ions, LC remained bright throughout the observation period and even further whereas at 75 nM of Pb^{2+} , it turned dark within 5-10 minutes. (Fig. 8) This suggests that the LC sensor is highly selective towards Pb^{2+} ions and does not show orientation change in the presence of other ions.

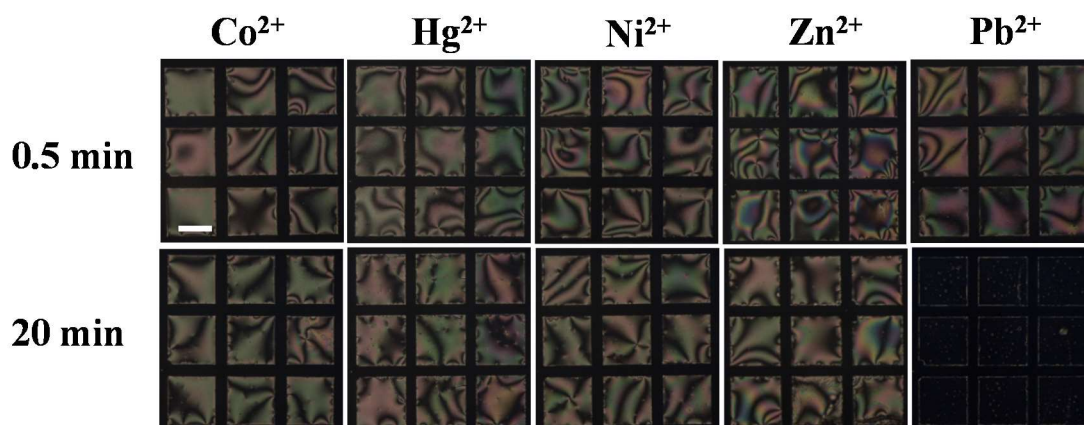


Figure 8. POM images of 5CB in gold TEM grid on DMOAP coated glass slide after introduction of 75 nM pre-incubated Co^{2+} , Hg^{2+} , Ni^{2+} , Zn^{2+} and Pb^{2+} , 7 μM CTAB and 200 nM SRNA. Scale bar = 200 μm .

The average gray scale intensity plot further demonstrates the selectivity of the biosensor towards Pb^{2+} ions. The average gray scale intensity remains highest in presence of other metal ions whereas it drops to minimum in the presence of Pb^{2+} ions. (Fig. 9A) The average *GI* plot of time lapse images demonstrate that with other metal ions, the *GI* remains almost constant, on the other hand with Pb^{2+} it decreases with time, finally achieving a minimum. (Fig. 9B)

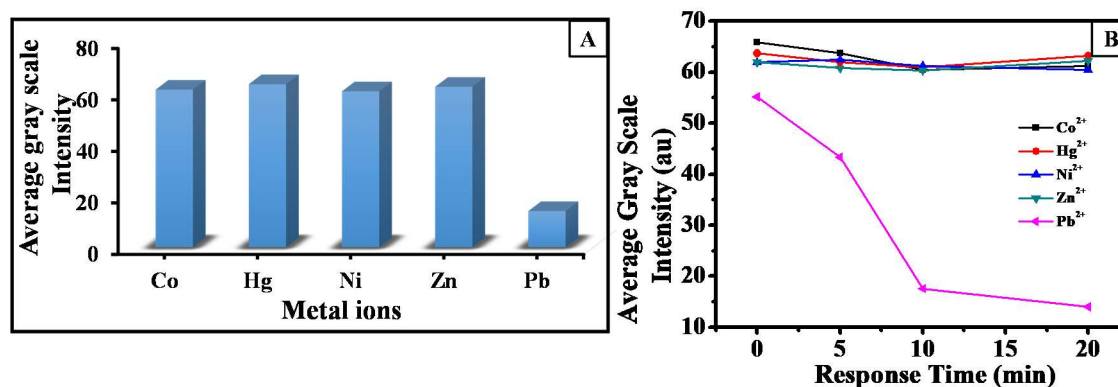


Figure 9. (A) Plot showing correlation between 75 nM concentration of different metal ions and average gray scale intensity after 20 minutes of addition of solution. (B) Graph representing average gray scale intensity vs time for different metal ions.

2.6 Specificity of the sensor towards aptamer

In the next set of experiments, we intended to examine the specificity of the aptamer towards Pb^{2+} ions. For this, we employed a random RNA aptamer sequence with a similar number of nucleobases and observed the response of the system with 150 nM of Pb^{2+} ions. We observed that in the case of a random RNA sequence, the LC exhibited a planar orientation and hence remained bright even after 30 minutes whereas in the case of SRNA aptamer the LC turned dark in less than 5 minutes and hence exhibited homeotropic orientation. (Fig. 10) This clearly suggests that the Pb^{2+} ions specifically bind with the SRNA aptamer and the LC exhibits distinct optical response when coupled with the Pb^{2+} - SRNA binding event.

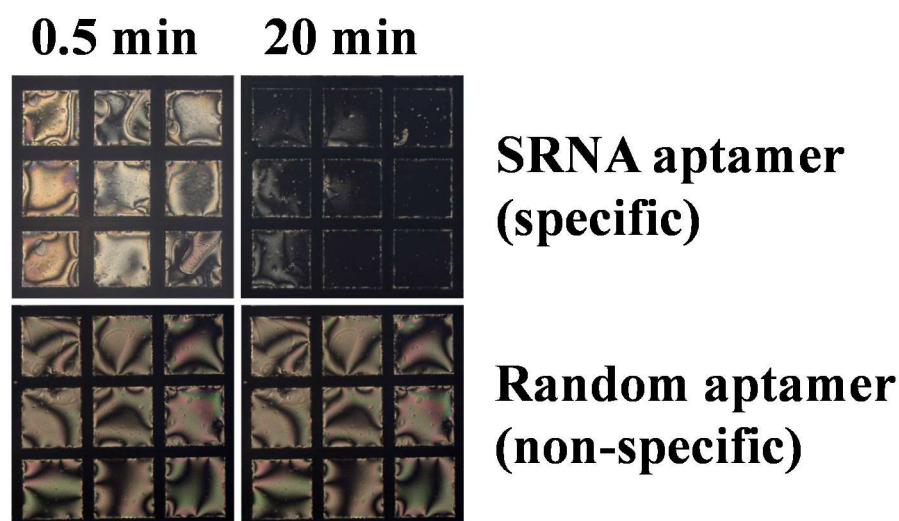


Figure 10. POM images of 5CB-aqueous interface laden with 7 μM CTAB and 150 nM Pb^{2+} with A) 200 nM SRNA aptamer sequence (specific) B) 200 nM random aptamer (non-specific).

2.8 Comparison with the existing methods of Pb^{2+} ion detection

To check how our proposed apta-LC sensor fares in comparison to the existing methods and detection limits, we analyze several previously reported methods of lead ion detection and contrast the strategies and detection limits. For these we compare our aptamer-LC based method with a range of techniques such as fluorescence³⁴⁻³⁶, calorimetry^{37, 38}, photo-electrochemical³⁹ and electrochemical⁴⁰. These techniques

require use of expensive instruments, fluorophores for labelling, and sensitive expert handling whereas the reported apta-LC sensor offers an easy visualization and simple, easy to handle, and label free technique for Pb^{2+} ion detection. Along with this our method provides an improved sensitivity with a detection limit of around 3 nM.

Chapter 3

Summary & Conclusions

3.1 Conclusion

3.2 Future Outlook

Conclusion

We have successfully developed a label free aptamer based LC sensor for Pb^{2+} ion detection. LCs being birefringent in nature have been employed several times to develop biosensors to detect different target analytes. But the previously reported sensors have limitation such as aptamer immobilization, poor selectivity and poor specificity. Here, in the reported work we have exploited the high affinity of the aptamers towards the target analyte to develop a sensor that is highly selective towards Pb^{2+} ions, shows specificity towards the SRNA and eliminates the need of aptamer immobilization. Along with this the sensor reported here also shows a low detection limit with the added advantage of easy solution preparation and equipment handling with easy to visualize results.

The CTAB being positively charged aligns the LC molecules homeotropically due to the hydrophobic interaction between the hydrocarbon chains of the surfactant and the LC. On addition of negatively charged SRNA, the self-assembly of the CTAB molecules at the interface gets disrupted and hence the LC turns bright, exhibiting a planar orientation. However, when Pb^{2+} ion is added in sufficiently high amount, the SRNA having specific affinity towards the Pb^{2+} ion, forms a stable G-quadruplex with the ion.³⁴ The formation of a G-quadruplex then disrupts the SRNA-CTAB interaction and hence the CTAB self assembles at the LC- aqueous interface imparting a homeotropic orientation to the LC and hence the LC appears dark. This provides an easy optical method for Pb^{2+} ion detection upto a concentration of 3 nM which is far less below the maximum permissible limit of 72 nM in potable water. Along with the excellent ability to detect low Pb^{2+} ion concentrations, the proposed biosensor also provides high selectivity towards Pb^{2+} ions with LC remaining bright with other common metal ions (Co^{2+} , Ni^{2+} , Hg^{2+} and Zn^{2+}) having a similar charge, radius and other properties. The system also shows a specificity towards the SRNA with the LC remaining bright in case of employing a random RNA aptamer sequence. This proves that the proposed biosensor provides an effective way of Pb^{2+} ion detection in the aqueous phase with excellent detection limit, high selectivity, specificity and easy sample preparation.

Future Outlook

The proposed design of biosensor, utilizing a Pb^{2+} specific aptamer to bring about change in the LC orientation can also be extended towards detection of other toxic metal ions by employing specific RNA/DNA aptamers. This easy to employ method might provide a gateway to utilize LC in detection of several other metal ions. Apart from this, the method can be extended to real time detection of Pb^{2+} ion concentration in the tap water sample indicating the applicability of the proposed biosensor towards addressing the easy detection of Pb^{2+} ion concentration in potable water and might be a small step in eradication of lead poisoning.

Bibliography

1. Collins, P. J.; Hird, M. *Introduction to Liquid Crystals Chemistry and Physics*, Taylor and Francis: London, **2009**, p.1-2, 9-10
2. Brake, J. M.; Abbott, N. L. An Experimental System for Imaging the Reversible Adsorption of Amphiphiles at Aqueous–Liquid Crystal Interfaces. *Langmuir* **2002**, *18*, 6101–6109.
3. Brake, J. M.; Daschner, M. K.; Luk, Y.-Y.; Abbott, N. L. Biomolecular Interactions at Phospholipid-Decorated Surfaces of Liquid Crystals. *Science* **2003**, *302*, 2094–2097.
4. Carlton, R. J.; Hunter, J. T.; Miller, D. S.; Abbasi, R.; Mushenheim, P. C.; Tan, L. N.; Abbott, N. L. Chemical and Biological Sensing using Liquid Crystals. *Liq. Cryst. Rev.* **2013**, *1*, 29–51.
5. Sidiq, S.; Pal, S. K. Liquid Crystal Biosensors: New Approaches. *Proc. Indian Natl. Sci. Acad.* **2016**, *82*, 75–98.
6. Popov, P.; Mann, E. K.; Jakli, A. Thermotropic Liquid Crystal Films for Biosensors and beyond. *J. Mater. Chem. B* **2017**, *5*, 5061–5078.
7. Kleman, M.; Lavrentovich, O. D. *Soft Matter Physics: An Introduction*; Springer: New York, **2003**.
8. de Gennes, P. G.; Prost, J. *The Physics of Liquid Crystals*; Clarendon Press: Oxford, **1993**.
9. Price, A. D.; Schwartz, D. K. DNA Hybridization-Induced Reorientation of Liquid Crystal Anchoring at the Nematic Liquid Crystal/Aqueous Interface. *J. Am. Chem. Soc.* **2008**, *130*, 8188–8194.

10. Verma, I.; Sidiq, S.; Pal, S. K. Poly(l-lysine)-coated Liquid Crystal Droplets for Sensitive Detection of DNA and their Applications in Controlled Release of Drug Molecules. *ACS Omega* **2017**, *2*, 7936–7945.
11. Noonan, P. S., Roberts, R. H., Schwartz, K. Liquid Crystal Reorientation Induced by Aptamer Conformational Changes. *J. Am. Chem. Soc.* **2013**, *135*, 5183–5189.
12. McUmbler, C. A.; Noonam, P. S.; Schwartz, D. K. Surfactant–DNA Interactions at the Liquid Crystal–Aqueous Interface. *Soft Matter* **2012**, *8*, 4335–4342.
13. Sidiq, S.; Prasad, G. V. R. K.; Mukhopadhaya, A.; Pal, S. K. Poly(l-lysine)-Coated Liquid Crystal Droplets for Cell-Based Sensing Applications. *J. Phys. Chem. B* **2017**, *121*, 4247–4256.
14. Manna, U.; Zayas-Gonzalez, Y. M.; Carlton, R. J.; Caruso, F.; Abbott, N. L.; Lynn, D. M. Liquid Crystal Chemical Sensors That Cells Can Wear. *Angew. Chem. Int. Ed.* **2013**, *52*, 14011–14015.
15. Verma, I.; Sidiq, S.; Pal, S. K. Protein Triggered Ordering Transitions in Poly (L-Lysine) Coated Liquid Crystal Emulsion Droplets. *Liquid Crystals* (Accepted for publication)
16. Das, D.; Sidiq, S.; Pal, S. K. A Simple Quantitative Method to Study Protein–Lipopolysaccharide Interactions by Using Liquid Crystals. *ChemPhysChem* **2015**, *16*, 753–760.
17. Seo, J. M.; Khan, W.; Park, S.-Y. Protein Detection using Aqueous/LC Interfaces Decorated with a Novel Polyacrylic Acid Block Liquid Crystalline Polymer. *Soft Matter* **2012**, *8*, 198–203.
18. Pani, I.; Sharma, D.; Pal, S. K. Liquid Crystals as Sensitive Reporters of Lipid-Protein Interactions. *General Chemistry* **2018**, *4*, 180012–180012.

19. Popov, P.; Honaker, L. W.; Kooijman, E. E.; Mann, E. K.; Jákli, A. I. A Liquid Crystal Biosensor for Specific Detection of Antigens. *Sens Biosensing Res.* **2016**, *8*, 31–35.
20. Lee, K.; Gupta, K. C.; Park, S.-Y.; Kang, I.-K. Anti-IgG-Anchored Liquid Crystal Microdroplets for Label Free Detection of IgG. *J. Mater. Chem. B* **2016**, *4*, 704–715.
21. Bai, Y.; Abbott, N. L.; Recent Advances in Colloidal and Interfacial Phenomena involving Liquid Crystals *Langmuir* **2011**, *27*, 5719–5738
22. Bi, X.; Hartono, D.; Yang, K.-L. Real-time Liquid Crystal pH Sensor for monitoring Enzymatic Activities of Penicillinase. *Adv Funct Mater.* **2009**, *19*, 3760–3765.
23. Verma, I.; Sidiq, S.; Pal, S. K. Detection of Creatinine using Surface-Driven Ordering Transitions of Liquid Crystals. *Liq. Cryst.* **2016**, *43*, 1126–1134.
24. Carlton, R. J.; Gupta, J. K.; Swift, C. L.; Abbott, N. L. Influence of Simple Electrolytes on the Orientational Ordering of Thermotropic Liquid Crystals at Aqueous Interfaces. *Langmuir* **2012**, *28*, 31–36.
25. Singh, S. K.; Nandi, R.; Mishra, K. Singh, H. K.; Singh, R. K.; Singh, B. Liquid Crystal Based Sensor System for the Real Time Detection of Mercuric Ions in Water using Amphiphilic Dithiocarbamate. *Sens. Actuator B-Chem* **2016**, *226*, 381–387.
26. Hu, Q.-Z.; Jang, C. H. Liquid Crystal-Based Sensors for the Detection of Heavy Metals using Surface-Immobilized Urease. *Colloids Surf. B* **2011**, *88*, 622–626.
27. Yang, S.; Wu, C.; Tan, H.; Wu, Y.; Liao, S.; Wu, Z.; Shen, G.; Yu, R. Label-Free Liquid Crystal Biosensor Based on Specific Oligonucleotide Probes for Heavy Metal Ions. *Anal. Chem.* **2013**, *85*, 14–18.
28. Thiviyanathan, V.; Gorenstein, D. G. Aptamers and the Next Generation of Diagnostic Reagents. *Proteomics Clin. Appl.* **2012**, *6*, 563–573.
29. Liu, J. W.; Cao, Z. H., Lu, Y. Functional Nucleic Acid Sensors. *Chemical Reviews* **2009**, *109*, 1948–1998.

30. Chen, P.; Greenberg, B.; Taghavi, S.; Romano, C.; Lelie, D.; He, C. An Exceptionally Selective Lead (II)-Regulatory Protein from *Ralstonia Metallidurans*: Development of a Fluorescent Lead (II) Probe. *Angew. Chem., Int. Ed.* **2005**, *44*, 2715–2719.
31. Kim, Y.; Johnson, R. C.; Hupp, J. T. Gold Nanoparticle-Based Sensing of “Spectroscopically Silent” Heavy Metal Ions. *Nano Lett.* **2001**, *1*, 165–167.
32. Devi, M.; Dhir, A.; Pradeep, C. P. Modulating Sensitivity and Detection Mechanism with Spacer Length: A New Series of Fluorescent Turn on Chemodosimeters for Pb²⁺ Based on Rhodamine–Quinoline Conjugates. *RSC Adv.* **2016**, *6*, 112728–112736.
33. http://www.who.int/water_sanitation_health/dwq/chemicals/lead.pdf Accessed: November, 2018
34. Gupta, S. D.; Shelke, S. A.; Li, N. S.; Piccirilli, J. A. Spinach RNA Aptamer Detects Lead(II) with High Selectivity. *Chem. Commun.* **2015**, *51*, 9034–9037.
35. Guo, L.; Nie, D.; Qiu, C.; Zheng, Q.; Wu, H.; Ye, P.; Hao, Y.; Fu, F.; Chen, G. A G-Quadruplex Based Label-Free Fluorescent Biosensor for Lead Ion. *Biosens. Bioelectron.* **2012**, *35*, 123–127.
36. Li, T.; Dong, S.; Wang, E. A Lead (II)-Driven DNA Molecular Device for Turn-On Fluorescence Detection of Lead (II) Ion with High Selectivity and Sensitivity. *J. Am. Chem. Soc.* **2010**, *132*, 13156–13157.
37. Li, T.; Wang, E.; Dong, S. Lead(II)-Induced Allosteric G-Quadruplex Dnazyme as a Colorimetric and Chemiluminescence Sensor for Highly Sensitive and Selective Pb²⁺ Detection. *Anal. Chem.* **2010**, *82*, 1515–1520.
38. Wang, Z.; Chen, B.; Duan, J.; Hao, T.; Jiang, X.; Guo, Z.; Wang, S. A Test Strip for Lead(II) Based on Gold Nanoparticles Multi-Functionalized by DNazyme and Barcode DNA. *J. Anal. Chem.* **2015**, *70*, 339–345.

39. Wang, G.-L.; Gu, T.-T.; Dong, Y.-M.; Wu, X. M.; Li, Z. J. Photoelectrochemical Aptasensing of Lead(II) Ion Based on the in Situ Generation of Photosensitizer of a Self-Operating Photocathode. *Electrochem. Commun.* **2015**, *61*, 117–120.
40. Bala, A.; Pietrzak, M.; Górski, L.; Malinowska, E. Electrochemical Determination of Lead Ion with DNA Oligonucleotide-Based Biosensor using Anionic Redox Marker. *Electrochim. Acta* **2015**, *180*, 763–769.